International Journal of Precision Engineering and Manufacturing
https://doi.org/10.1007/s12541-019-00151-8

Online ISSN 2005-4602
Print ISSN 2234-7593

REGULAR PAPER

A Geometric Error Modeling Method and Trajectory Optimization Applied in Laser Welding System

Hao Tang[1] · Zilin Zhang[1] · Changping Li[1] · Tae Jo Ko[1,2]

Received: 7 November 2018 / Revised: 14 April 2019 / Accepted: 7 May 2019

Abstract

In this paper, a geometric error modeling method is carried out on six-axis motion platform (SMP) in laser welding system (LWS), and an optimized algorithm is proposed for the alignment in LWS based on the error model. First, the topological structure of the given SMP is analyzed, and related homogeneous transformation matrices which are used for standing the orientation of SMP are established. By these matrices, the geometric error model is developed mathematically. Then, the error model is used for predicting the alignment deviations. A corresponding series of experiments for calculating the optical power loss in alignment are employed, and the comparison between simulation and experiments results indicate the validation of the error model. Furthermore, an optimized algorithm is applied to search the optimum aligning trajectory. Compared to conventional method, this algorithm has a broader range in searching extreme value, which can reduce the computational volume and improve the efficiency. It is also beneficial for improving the success rate of escaping from the local minimum spot and finding the optimum alignment spot. The error model is helpful to analyze the error propagation process and improve the alignment efficiency in LWS, which can be applied to other similar multi-axis precise system.

Keywords Six-axis motion platform · Error modeling · Trajectory optimization · Alignment algorithm · Laser welding system

List of Symbol

SMP	Six-axis motion platform
MMS	Multi-axis motion system
MMP	Multi-axis motion platform
OD	Optical device
LWS	Laser welding system
B	Typical body
X, Y, Z, U, V, W	Axis in MMS
$x, y, z, \alpha, \gamma, \beta$	Geometric error
T	Intersubject transformation matrix
E	Error matrix of homogeneous transformation
$\boldsymbol{T}_s$	Intersubject coordinate offset matrix
$\boldsymbol{E}_s$	Motion transformation matrix
$\boldsymbol{T}_k^s$	Kinematic error matrix
$\boldsymbol{E}_k^s$	Static error matrix
LD	Laser diode
SMF	Single-mode optical fiber
PL	Power loss
EMM	Error modeling method
EMSM	Error modeling searching method

✉ Hao Tang
tanghao@hnust.edu.cn

[1] School of Mechanical Engineering, Hunan University of Science and Technology, Xiangtan 411201, Hunan, China

[2] School of Mechanical Engineering, Yeungnam University, Gyeongsan 712-749, Korea

1 Introduction

Optoelectronic devices (OD) [1, 2] manufacture, indispensable to telecommunication industry and all-optical communication network construction, are commonly utilized in the advanced researches and engineering industries. Generally, the quality of OD device is relied on the packaging accuracy. At present, the most common tool to package OD is laser welding system (LWS) [2]. This system is constituted by a detection unit and an alignment unit, and the Alignment unit is the core unit of LWS. As the most important component in this core unit, the multi-axis motion platform (MMP) determines the accuracy of optical devices' packaging. To achieve high quality in OD packaging process, errors produced during movements on MMP need to be as lower as possible. There are some

Published online: 22 May 2019

discussions and researches about efficiency improvement through algorithm on alignment trajectory searching [3–5]. However, few studies have been made aimed at this issue by using the error modeling method.

MMP is a special kind of multi-axis motion system (MMS) [4, 5] which is extensively adopted in manufacturing industry and robotics research [6]. This system is normally required of high precision and accuracy control. From micro perspective, inaccuracy of this system is mostly resulted from geometric error, thermal error [7], static and dynamic loading error and mismatches between servo-loop parameters etc. [5, 8]. All error sources affect the accuracy of MMS in complex ways. The contributions of different error sources to volumetric errors of machine tools had been discussed by Andolfatto [9]. MMP [10, 11] is widely utilized in engineering regions such as in optoelectronic packaging system. In MMP, the impact of geometric errors weight heavily on pose accuracy among the abovementioned errors [11, 12]. To know it further, a suitable way for analyzing multi-body system and for developing an error compensation [13] scheme is introduced named error modeling [14, 15]. Error modeling method (EMM) can be used to predict deviations during machine operation, which is closely related to the identification of precision level of MMP. Thus, by using this method comprehensive error analysis can be constructed to achieve high-accuracy in MMP.

EMM not only can calculate the conventional errors which affect system's precision, but also can be a useful approach to assess the quality and efficiency for MMS. This method is usually used in machine tools (a typical multi-body system), such as CNC machine tools and 3-dimensional measurement machine. For instance, an error model [16] based on EMM for a four-axis machine tool is constructed to research the tool pose error with geometric error parameters and to calculate error propagation, also the key errors are analyzed. Cheng [17] proposed a novel analytical method on the basis of EMM for geometric errors identification of multi-axis machine tool, which can not only identify crucial geometric errors, but the stochastic and intercoupling characteristics of the geometric errors are also considered. Lee [18] made analysis on a five-axis machine tool with general orthogonal configuration and concluded that the machining accuracy can be improved by adjustment of each component's size or by reduction of moving distance on mobile axes. However, there are few researches about using this method on MMP. This method has been proved a feasible way to analyze the pose variation of CNC machine tools. It should also be included when evaluating the MMP in LWS. Therefore the EMM is tested in the analysis of the accuracy of LWS in this paper. Besides, the results of this analysis will be used as an auxiliary reference to developing aligning algorithm for such systems.

Conventional aligning algorithms [19], for example, the hill climbing method, Hamiltonian path method, the adaptive optimization method and the pattern search method are often used to find the optimized trajectory of alignment during machine operation [20–22]. But few studies have been done on using these aligning algorithms to predict optimized trajectories for MMP. Besides, concerning the high accuracy of a control system, many scholars did experiments on already build-up platforms to evaluate and compensate errors based on EMM, but few considered used it to predict the aligning trajectory for LWS. Chun [19] had compared 3 aligning algorithms in many different respects, like coupling velocity and success rate, and utilized these algorithms in laser welding operation. Aguado [23] not only identified geometrical error parameters for machining tools, The distribution of measurement points, mesh or cloud, and optimization constraints of polynomial regressions which also affect machine tools accuracy were studied. And a compensation about these factors was applied. In a similar approach, a geometric and thermal comprehensive error model was built and an error compensation method was discussed by Zhang [24] to improve the machining precision for four-axis polishing platforms. However, these scholars did not consider using these methods in a novel perspective. In this paper, a new aligning algorithm based on error modeling is proposed and explained. Also it will be evaluated with a comparison algorithm, pattern search method. Simulations will be made by using these two algorithms with EMM, the results of which can predict the optimized trajectory for alignment and also can be used as criteria for assessment of the quality of LWS.

2 Error Modeling Method

A mechanical system, which is called multi-body system [25], consists of several multiple rigid bodies and flexible multi-body interconnected to each other in a certain way. In order to analyze the working state of multi-body system, a mathematical description way is adopted. Topological structure, as a simulation approach for various connection and structures of normal multi-body system, is widely used in machine tools and CNC manufacture center. By building topological structure, a traditional error modeling method can be introduced into this paper to calculate the comprehensive systematic orientation error to assess if the deviation has gone beyond the threshold. By doing further sensitivity analysis, this method can be used to distinguish key errors and design an error compensation system aimed at these parameters.

The ideal coordinates of units installation of a MMS is drawn in black in Fig. 1, the real coordinates is drawn in red. The static errors which are derived from assembly error [26] and coordinate offsets are illustrated in Fig. 1. From

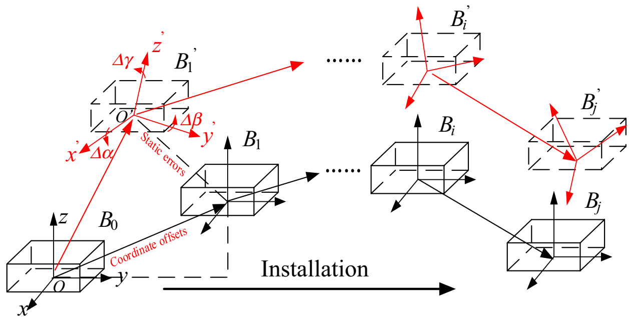

Fig. 1 Static errors generated during the platforms' installation

Table 1 Characteristic matrices between two adjacent units

Intersubject coordinate offset matrix	Static error matrix
$T_s = \begin{bmatrix} 1 & 0 & 0 & x_s \\ 0 & 1 & 0 & y_s \\ 0 & 0 & 1 & z_s \\ 0 & 0 & 0 & 1 \end{bmatrix}$	$E_s = \begin{bmatrix} 1 & \Delta\gamma_s & \Delta\beta_s & 0 \\ \Delta\gamma_s & 1 & -\Delta\alpha_s & 0 \\ -\Delta\beta_s & \Delta\alpha_s & 1 & 0 \\ 0 & 0 & 0 & 1 \end{bmatrix}$
Motion transformation matrix	**Kinematic error matrix**
$T_k^x = \begin{bmatrix} 1 & 0 & 0 & 0 \\ 0 & \cos\alpha_k^x & -\sin\alpha_k^x & 0 \\ 0 & \sin\alpha_k^x & \cos\alpha_k^x & 0 \\ 0 & 0 & 0 & 1 \end{bmatrix}$	$E_k^x = \begin{bmatrix} 1 & \Delta\gamma_k^x & \Delta\beta_k^x & \Delta x_k^x \\ \Delta\gamma_k^x & 1 & -\Delta\alpha_k^x & \Delta y_k^x \\ -\Delta\beta_k^x & \Delta\alpha_k^x & 1 & \Delta z_k^x \\ 0 & 0 & 0 & 1 \end{bmatrix}$

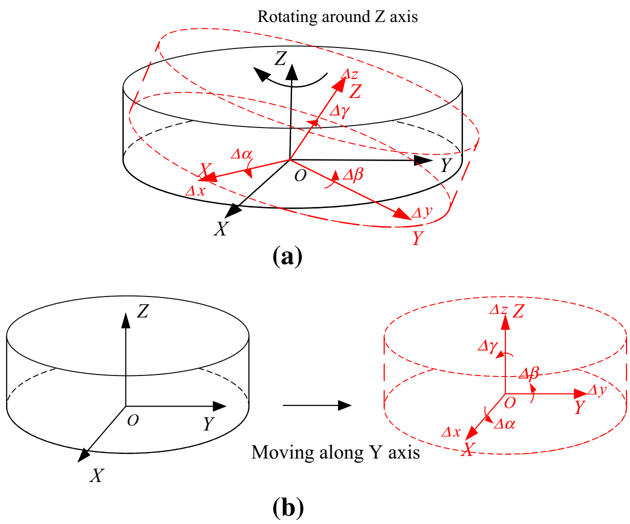

Fig. 2 Kinematic errors generated in two types of motion. **a** Kinematic errors generated in rotational movement around Z axis, **b** kinematic errors generated in translational movement along Y axis

this figure, B denotes body, subscript denotes the installation serial number of different bodies. Superscript represents the real state of various bodies. According to the lower body array description for the topological structure of MMS, the relation between B_i and B_j *is* $L^n(j)=i$, which means B_i is the n-order lower body of B_j. From Fig. 2, there are deviations of 6 degree of freedom generated in two types of motion. These deviations are represented by kinematic errors. To describe the motion propagation [27] and error flow of MMS in mathematical model, the lower body description is utilized and associated with 4×4 homogeneous matrix method.

Table 1 presents the typical transmission matrices for error flow analysis, which is described in rigid body kinematics [4]. Where, subscript s denotes static phase, and k denotes kinematic phase. Superscript is the axis of motion in kinematic phase of each part. For instance, T_k^x means kinematic transformation matrix orientation movement around X axis. The matrices in Table 1 are based on a rotation motion around X axis.

Taking the coordinate of B_i to be the references coordinate of B_j, B_j move along X axis, the ideal and actual pose matrices of B_j are presented:

$$P_{Ij} = T_s \cdot T_k^x \cdot V_j \tag{1}$$

$$P_{Rj} = T_s \cdot E_s \cdot T_k^x \cdot E_k^x \cdot V_j \tag{2}$$

where V_j is a vector that begins in a fixed point in B_0 and ends in a fixed point in B_j for pose measurement. P_{Ij} denotes the ideal orientation of B_j, P_{Rj} denotes the real orientation of B_j. The deviation between the pose of physical operation and the pose of ideal situation can be analyzed by the difference of P_{Ij} and P_{Rj}. The relative error matrix of B_j generated during displacement is shown below:

$$E_j = P_{Rj} - P_{Ij} \tag{3}$$

Considering the ground coordinate which is set on B_0 as reference coordinate, the deviation of B_j between ideal and real routes is the difference of P_I and P_R. The orientation matrix of P_I and P_R should both be deduced by the combination of preceding intersubject homogeneous transformation matrices. P_I and P_R are shown as follows,

$$P_R = \prod_{M=N,L^N(X)=0}^{M=1} T_{L^N(X)L^{N-1}(X)S} \cdot \Delta T_{L^N(X)L^{N-1}(X)S} \cdot T_{L^N(X)L^{N-1}(X)K} \cdot \Delta T_{L^N(X)L^{N-1}(X)K} \cdot V_j \tag{4}$$

$$P_I = \prod_{M=N,L^N(X)=0}^{M=1} T_{L^N(X)L^{N-1}(X)S} \cdot T_{L^N(X)L^{N-1}(X)K} \cdot V_j \tag{5}$$

3 Error Modeling on Six-Axis Motion Platform in LWS

LWS is utilized for optical device manufacturing industry. Generally, it consists of two modules, as Fig. 3 shows, aligning sub-system and detecting sub-system. Aligning sub-system is composed of lower and upper components

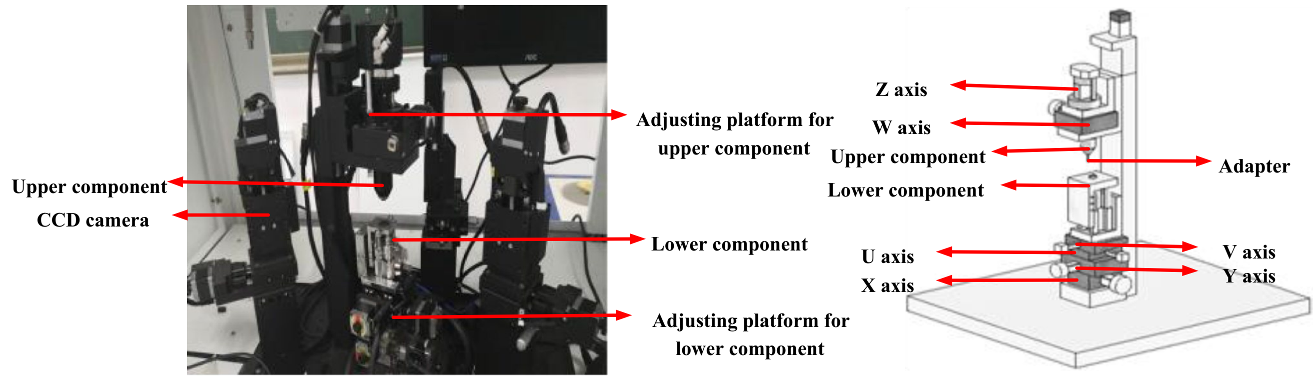

Fig. 3 Model and schematic of SMP in LWS

Table 2 Spec of translational motion platform in LWS

Travel range (mm)	30
Resolution: full(pulse) (μm)	1
Resolution: half(pulse) (μm)	0.5
Resolution: micro step 1/20 split(pulse) (μm)	0.05
Lost motion (within μm)	1
MAX. speed (mm/s)	10
Uni-directional positioning accuracy (within μm)	5
Repeatability positioning accuracy (within ± μm)	0.3
Backlash (within μm)	0.5

Table 3 Spec of rotational motion platform in LWS

Travel range (±°)	360
Resolution: full(pulse) (°)	0.006
Resolution: half(pulse) (°)	0.003
Lost motion (within °)	0.05
MAX. speed (°/s)	30
Uni-directional positioning accuracy (within °)	0.05
Repeatability positioning accuracy (within ± °)	0.01
Backlash (within °)	0.1

which are controlled by 6-axis motion platform. Parameter details of 6-axis motion platform in LWS are presented in Tables 2 and 3, which are taken from the company handbook [28]. Detecting sub-system is composed of three cameras to omnibearingly detect the poses of optical products. The geometric errors, a set of parameters generated during the platform operation are overwhelmingly beyond other errors. They will cause inaccurate alignment which results in the loss of optical coupling efficiency to affects the quality of OD. Therefore, the analysis based on error modeling of alignment sub-system and research on how to improve the coupling efficiency are the main topics in the assessment of LWS.

In Fig. 3, this SMP consists of 3 translational platforms named X, Y, Z and 3 rotational platforms named U, V, W respectively, and a coupling unit which is made of 2 main parts, the upper and lower component. Because of the orientation of the coupling unit is controlled by the SMP, the precision level of motion platform determines the aligning accuracy. The topological structure of this system and generalized coordinates on every typical unit are illustrated in Fig. 4. The pose deviation between coupling parts P_5 and P_9 is illustrated. P means part in Fig. 4.

In the alignment operation of single mode fiber (SMF) and laser diode (LD), comprehensive errors are propagated from ground unit to optical components. In this paper, SMF is fixed in P_5 part, LD is fixed in P_9 part. As Fig. 5 shows, the alignment deviations between SMF and LD are illustrated in detail. In order to evaluate the accuracy of coupling unit, firstly two fixed points are set on SMF and LD respectively to observe the position variation. Then two fixed vectors are set on SMF and LD separately as well to observe the pose variation. The poses and positions of SMD and LD can be deduced by Eqs. (4) and (5). Therefore the differences between the real poses, positions of SMF and those of LD can be derived by differencing the actual state matrices of two alignment parts.

Setting $\vec{V}$ as a vector in P_5 coordinate, V as a point in P_5 coordinate. Setting $\vec{U}$ as a vector in P_9 coordinate, U as a point in P_9 coordinate. Therefore the real poses and positions of P_5 and P_9 can be calculated, the space error model between these 2 parts are given as follows:

$$\overrightarrow{P_{5R}} = \prod_{M=N, L^N(5)=0}^{M=1} T_{L^N(5)L^{N-1}(5)S} \cdot \Delta T_{L^N(5)L^{N-1}(5)S} \cdot T_{L^N(5)L^{N-1}(5)K} \cdot \Delta T_{L^N(5)L^{N-1}(5)K} \cdot \vec{V} \tag{6}$$

$$\overrightarrow{P_{9R}} = \prod_{M=N,L^N(9)=0}^{M=1} T_{L^N(9)L^{N-1}(9)S} \cdot \Delta T_{L^N(9)L^{N-1}(9)S} \cdot T_{L^N(9)L^{N-1}(9)K} \cdot \Delta T_{L^N(9)L^{N-1}(9)K} \cdot \vec{U} \tag{7}$$

$$\vec{E} = \overrightarrow{P_{9R}} - \overrightarrow{P_{5R}} \tag{8}$$

$$P_{5R} = \prod_{M=N,L^N(5)=0}^{M=1} T_{L^N(5)L^{N-1}(5)S} \cdot \Delta T_{L^N(5)L^{N-1}(5)S} \cdot T_{L^N(5)L^{N-1}(5)K} \cdot \Delta T_{L^N(5)L^{N-1}(5)K} \cdot V \tag{9}$$

$$P_{9R} = \prod_{M=N,L^N(9)=0}^{M=1} T_{L^N(9)L^{N-1}(9)S} \cdot \Delta T_{L^N(9)L^{N-1}(9)S} \cdot T_{L^N(9)L^{N-1}(9)K} \cdot \Delta T_{L^N(9)L^{N-1}(9)K} \cdot U \tag{10}$$

$$E = P_{9R} - P_{5R} \tag{11}$$

$\vec{E}$ denotes the pose deviation from $\overrightarrow{P_{9R}}$ to $\overrightarrow{P_{5R}}$, $\overrightarrow{P_{9R}}$ denotes the real pose of P_9 component, and $\overrightarrow{P_{5R}}$ represents the real pose of P_5 component. E denotes the position deviation from P_{9R} to P_{5R}, P_{9R} denotes the real position of P_9 component, and P_{5R} represents the real position of P_5 component. Both E and $\vec{E}$ can be the criteria to evaluate the accuracy of alignment.

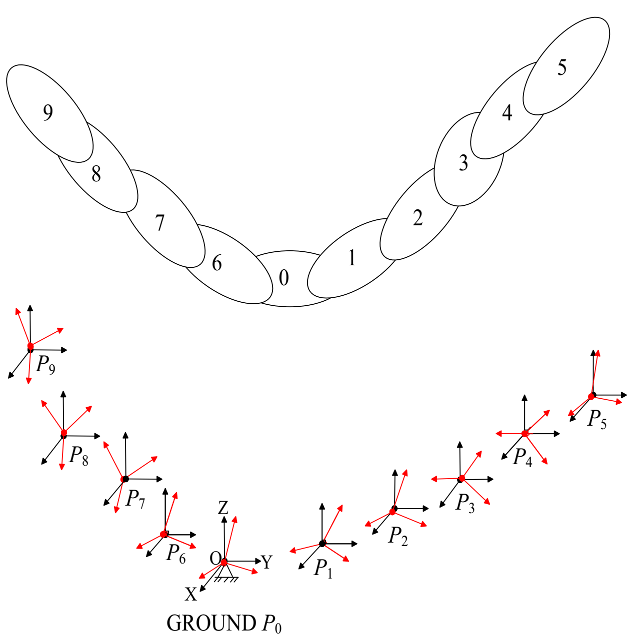

Fig. 4 Topological structure and generalized coordinates of SMP

4 A Novel Algorithm for Alignment

In Chun's [19] paper, 1 coarse registration algorithm and 3 fine registration algorithms had been discussed. He pointed

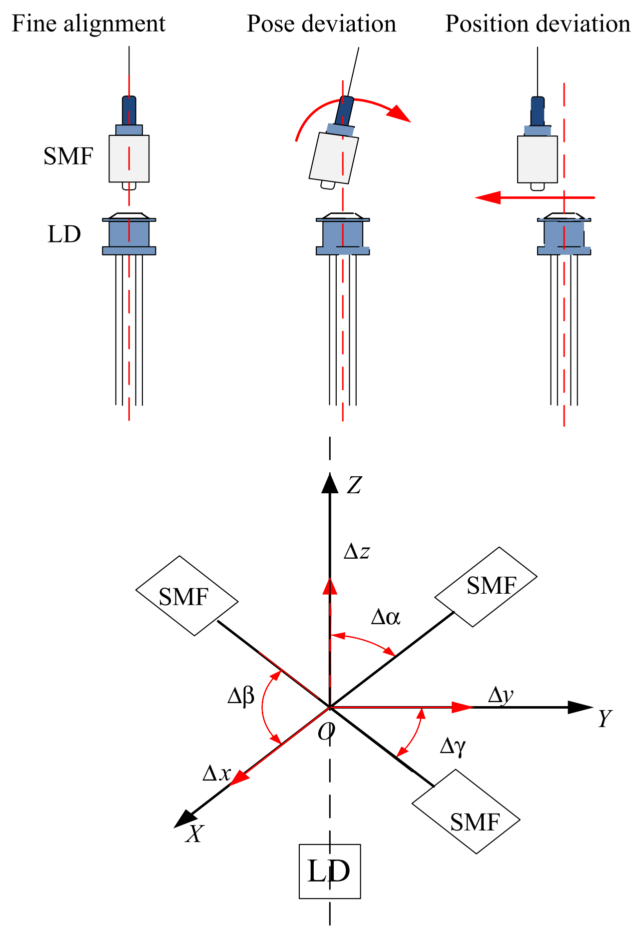

Fig. 5 Coupling errors between laser diode (LD) and single mode fiber (SMF) fixtures in alignment

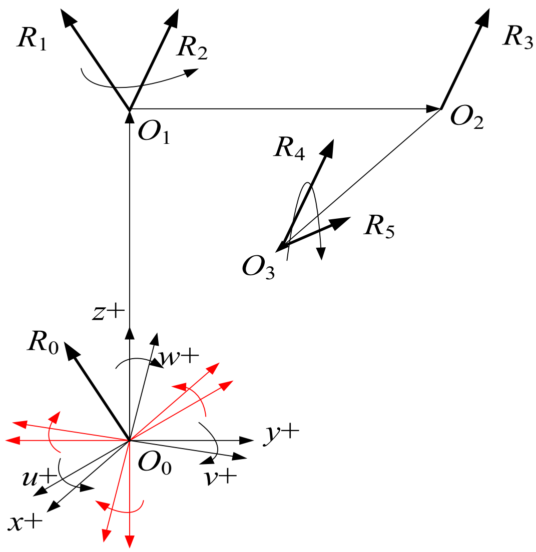

Fig. 6 Trajectory searching concept of EMSM

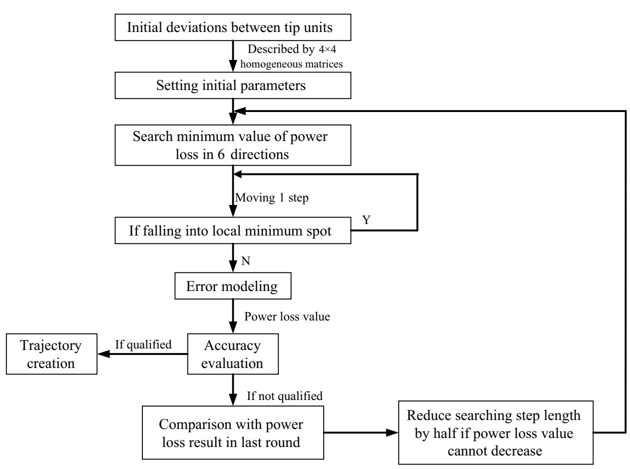

Fig. 7 Flow chart of error modeling searching method

out that pattern search method not only saves time but also has the highest success rate on the premise of high-precision controlling system. Based on this, all the algorithms are demonstrated based on the experiment results, which means these algorithms were only utilized in trajectory searching of actual operation.

In this paper, by using EMM, a novel aligning method is proposed, named as error modeling searching method (EMSM). This method can predict the optimized alignment trajectory with given message of the initial orientations of alignment parts or the initial deviations between the alignment parts in a reference coordinate. EMSM searches trajectories in 6-degree of freedom, pattern search method also search routes in multi-degree of freedom motion directions. Also by using EMM, both algorithms can be utilized to do trajectory prediction. Therefore, to evaluate the performance of EMSM, pattern search method will be compared with EMSM in this paper.

The concept of this algorithm is shown in Fig. 6. Where, R means a random vector, the initial state of R is R_0, R_i means the i state of vector R. This method has combined coarse alignment functions with fine alignment functions, which means this algorithm can be used in a broad range of initial misalignment if the initial power loss value of alignment parts is detectable or computable. The algorithm procedure is depicted in Fig. 7,

1. Select a reference coordinate, and find the initial deviation between alignment parts or the orientations of alignment parts. Set initial 4×4 matrices to describe them.
2. Set an initial step length, and search 6-degree of freedom directions and find the minimum value of power loss in 6 directions. Move SMP by one step in this direction, and set this minimum value spot as moving part's new origin point. Then update the new orientations of alignment parts.
3. Search the minimum value again in the new spot. If the power loss values in 6 directions are larger than the power loss value in its origin point without exception, i.e. alignment parts have gone into a local minimum spot, increase searching motion to 2 steps and search again. If the results are still not satisfied, the searching motion will be increased by 1 step at a time until the moving parts escape from the local minimum spot.
4. If the power loss value cannot decrease but the deviation is still below the standard, in this paper which means the value of power loss is over 1 dB, reduce the initial searching step length by half and repeat procedure 1 to 3 again until the result meets the threshold requirement.
5. If the final result has met the requirement, or the power loss value is changed negative, stop searching. The last minimum spot is the fine alignment location, and the last poses of alignment parts are the fine alignment poses.

Emphasis The initial step length should be larger than 1 μm. In that case, the chance to fall into local minimum will be lower and the number of increasing steps for jumping out of the local minimum will be reduced. The angular step length cannot be larger than 3°, usually set initial angular step length in the range from 0.02° to 0.06°.

In the pattern search method, the motion stage move in a certain sequence of multiple directions to search trajectory, which means this method starts searching from X positive direction, and then searches trajectory in Y and Z directions in order, and moves on to other directions. In contrast, EMSM only considers the fastest declining directions of power loss. Pattern search method has applied blind test thought by introducing accelerated factor in algorithm to raise aligning efficiency. Besides, in pattern search method, aligning units escape from local minimum by reducing step length. EMSM increases step numbers to achieve this task. Also the initial step length should be a bit larger in EMSM to realize coarse alignment. When the initial step length cannot meet the iteration requirements, reduce the step length to do fine alignment. Usually the initial step length is set under 10 μm when the initial power loss value of alignment units is under 1000 dB.

Table 4 Extreme value of each parameter

Value	Error, offsets and movements
0.1 μm	$u_x^R, u_y^R, u_z^R, u_v^R, u_w^R, v_x^R, v_y^R, v_z^R, v_u^R, v_w^R, w_x^R, w_y^R, w_z^R, w_u^R, w_v^R$
0.5 μm	$\alpha_x^P, \alpha_u^P, \alpha_{yv}^P, \alpha_{zw}^P, \beta_y^P, \beta_v^P, \beta_{xu}^P, \beta_{zw}^P, \gamma_w^P, \gamma_z^P, \gamma_{xu}^P, \gamma_{yv}^P$
1 μm	$x_y^T, x_z^T, x_u^T, x_v^T, x_w^T, y_x^T, y_z^T, y_u^T, y_v^T, y_w^T, z_x^T, z_y^T, z_u^T, z_v^T, z_w^T$
2 μm	x_x^T, y_y^T, z_z^T
3 μm	u_u^R, v_v^R, w_w^R
1 mm	Movement of each translational axis: X^T, Y^T, Z^T
20 mm	Offsets: $Y_z^c, Y_x^c, Y_w^c, Y_y^c, Z_y^c, Z_v^c, Z_u^c$
1°	Movement of each rotational axis: U^R, V^R, W^R

5 Case Study

5.1 Verification of Error Modeling on LWS

In order to evaluate the feasibility of error modeling in LWS, the results by using this method with given values of every motions and errors will be compared with the lab experimental results in this section.

To evaluate the quality of LWS, the extreme situation of deviations need to be considered. Then the results can be used to develop the assessment criteria. The extreme value of each parameter are given by the company handbook [28] (see Table 4), so that the simulated experiment referring Eqs. (6–11) is designed. In Table 4, Superscript R denotes rotational state, C denotes offsets, T denotes translational state, and P denotes position errors. Subscripts denote motion stages.

Before these simulations are conducted, the transform equations transforming from position and pose displacements to coupling efficiency and optical power loss value is given. PL denotes power loss.

$$\eta = \eta_x \eta_y \tag{12}$$

$$\eta_x = k \cdot exp\left\{ -k\left[\frac{d^2}{2}\left(1/\omega_{x0}^2 + 1/\omega_{f0}^2 \right) + \pi^2\theta^2\left[\omega_{x0}^2(z) + \omega_{f0}^2 \right]/2\lambda^2 - d\theta z/\omega_{x0}^2 \right] \right\} \tag{13}$$

$$\eta_y = k_y \cdot exp\left\{ -k_y\left[\frac{y^2}{2}\left(1/\omega_{y0}^2 + 1/\omega_{f0}^2 \right) + \pi^2\beta^2\left[\omega_{y0}^2(z) + \omega_{f0}^2 \right]/2\lambda^2 - y\beta z/\omega_{y0}^2 \right] \right\} \tag{14}$$

$$k = 4\omega_{x0}^2\omega_{f0}^2 \Big/ \left[(\omega_{x0}^2 + \omega_{f0}^2)^2 + \lambda^2 z^2/\pi \right]^2 \tag{15}$$

$$PL = -10 \cdot lg\, \eta \tag{16}$$

Figure 8 shows the general composition of experimental devices. The Optical power meter is used to collect power loss data which is to the criteria to assess the alignment

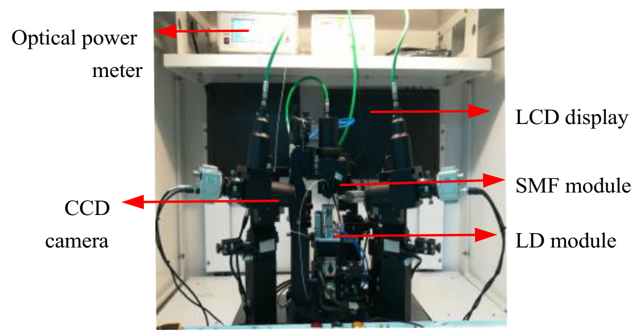

Fig. 8 Experimental installation of error modeling validation in LWS

quality. The CCD cameras are set vertically and horizontally. Other modules have been mentioned above in this paper.

In order to verify the accuracy of Error Modeling on LWS, a series of experiments are conducted on the laser welding machine. The alignment quality is more sensitive to the translational motions in X, Y directions and rotational movements around U, V axes compared to other fundamental movements. This essay only involve evaluation on translational displacements of X and Y axes. Also data of translational movements on Z axis should be collected as a contrast. Besides, the alignment tolerances for displacements on X and Y axes are 2 μm and 2.5 μm respectively [1]. The tolerance for Z axis is more than tenfold those of X and Y axes. Then the experiment is designed. Recording the power loss values at quintuple one pace and 8 sets of data in total. Then changing the direction to negative side, repeating the

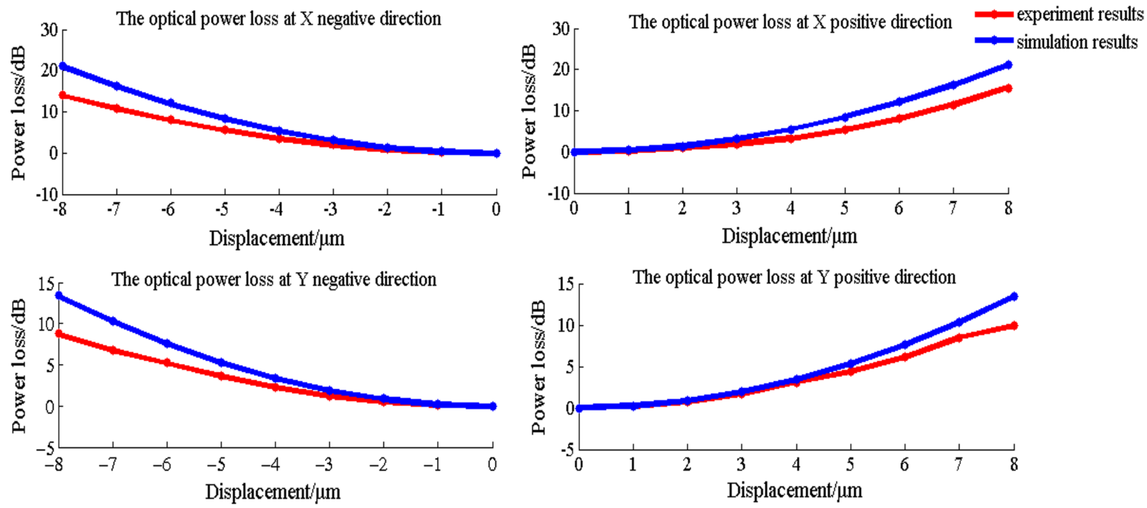

Fig. 9 The comparison between the experiments results and simulation results at *Y* and *X* stage

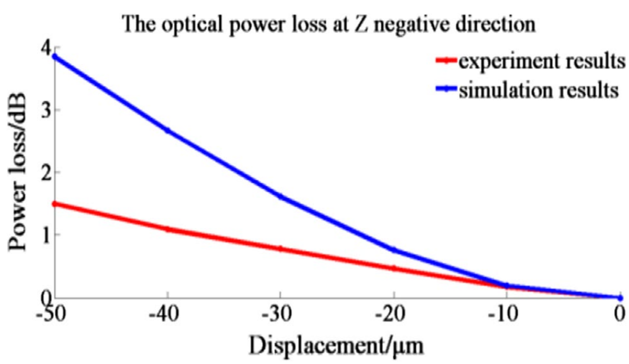

Fig. 10 The comparison between the experiment results and simulation results at *Z* stage

procedures. Doing the same experiments on *Y* stage again. The fifth experiment is performed in *Z* minus direction, and the displacement is 10 μm a time. Only recording 5 sets of data on that stage. The comparison between the results of experiments and simulations is illustrated in the line charts shown as Figs. 9 and 10.

It is noticeable that from the origin points of 4 graphs in Fig. 9, the deviations between experiment values and simulation values are negligible in the range of 2 μm displacement. But with the increase of displacement, the differences appear and become larger, while the trend of experiment results is similar to that of simulation results in *X* direction as well as in *Y* direction. In Fig. 10, for the experiment on *Z* stage, the variation is growing slowly, with unit displacement as tenfold the displacement on *X* stage and *Y* stage. It is also noticed that from the early paces, the figures for experiment overlap with the figures for simulation. By the comparison between the fifth chart and other 4 charts, the deviations for *Z* axis are tinier than the figures for *X* and *Y* axes. Also the trend of simulation value is generally the same to that of experiment result in *Z* minus axis.

For all the fact that this simulation is under the worst situation, the power loss gaps will be expanding with displacement increasing, the results are useful in the prediction of power loss pattern for different motion patterns. Also the results can be controlled under the specified amount to ensure the coupling accuracy in LWS. If more consideration is given in the disposal of the known information of different error values or more data is recorded and compensated, the results will be more precise and much nearer to each other. In another aspect, the power loss of *Y* axis motion is bigger than that of *X* axis motion under the same quantity of displacement. This case can be interpreted to that *X*-axis motion is less influential to the machine because the *X*-axis stage in this machine is a lower body to the *Y* stage. Therefore, how the lower body gives impact on the higher stages' orientation can be estimated effectively. These parameters accumulate part by part, which forms a great deviation in the end. From the final chart, it is deduced that the impact of movements along *Z* minus direction is insignificant compared to the impact of movements in other two axes.

Based on the discussions and conclusions, the further work of this research would be using iterative algorithm to search the optimum alignment trajectory and design the movement pattern for the laser welding machine, or based on a given trajectory to calculate the best installation sequence of motion platforms.

Table 5 Comparison between EMSM and pattern search method in several aspects

Trajectory planning algorithm	Searching times		Aligning time (s)	Alignment quality	Alignment range
	Success times	Failure times			
Pattern search method	28	2	2–4	Under 1 dB	Only fine alignment
EMSM	30	0	3–5	Under 1 dB	Course alignment and fine alignment

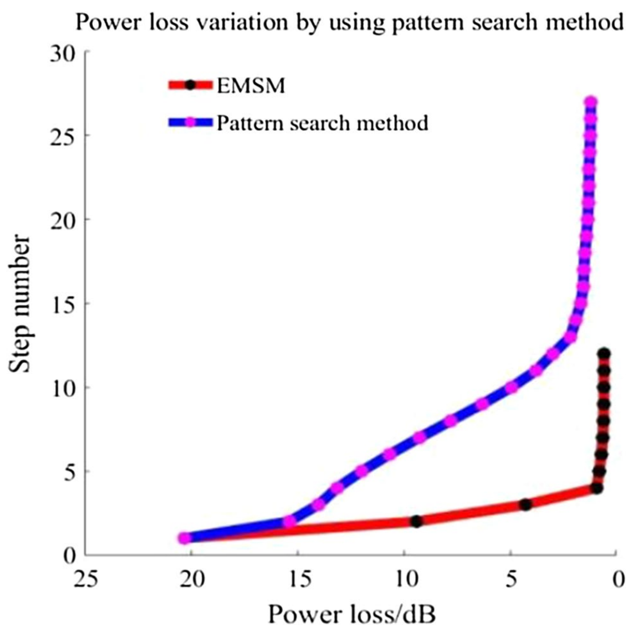

Fig. 11 Alignment simulation results with large initial deviations by using EMSM and pattern search method

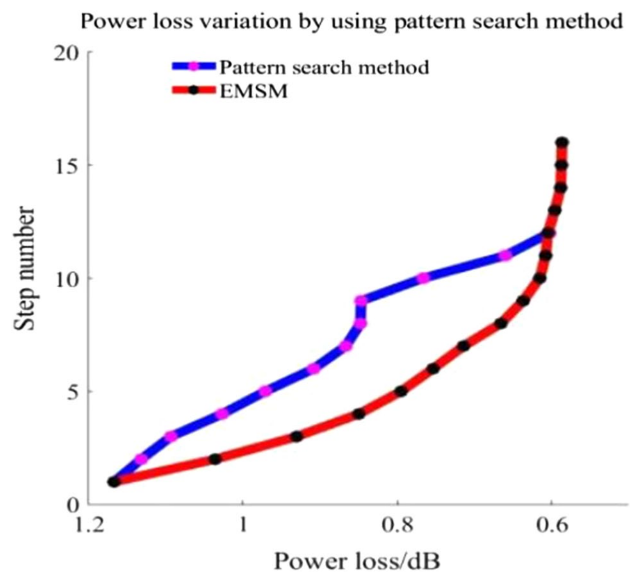

Fig. 12 Alignment simulation results with small initial deviations by using EMSM and pattern search method

5.2 Comparison of Performance Between EWSM and Pattern Search Method

The result of Sect. 5.1 indicates that error modeling method can be used for trajectory planning. Therefore the theory of EMSM mentioned in Sect. 4 is supported, to evaluate the quality of this method, pattern search method is introduced as reference standard. Pattern search method is assessed by many scholars and is demonstrated more efficient and accurate than other conventional alignment methods, such as mountain climbing method, parabola fitting method, etc. The basic idea of pattern search method is approaching maximum value of optical power in an iterative sequence in multiple degree-of-freedom. The comparison of performance between these two methods is given below.

This comparison is arrange by simulation experiments, therefore the influences of environmental condition are not considered, 30 random initial deviation matrices of alignment parts were chosen and a reference coordinate was selected to build 30 sets of orientations' matrices for alignment parts. Pattern search method and EMSM were utilized separately to do trajectory searching in 30 groups' comparison. For the results (see Table 5), pattern search method had successfully found the alignment path at 28 times, the searching procedure of 2 failure times have been tapped in local minimum spot. In contrast, EMSM had no failure in 30 simulations.

Beyond that, the results of this new method are very stable and very accurate, the results are under 1 dB. The results of pattern search method are mostly under 1 dB. Although pattern search method costs less time than EMSM when simulating, it is noticeable that this new method is as accurate as pattern search method and have higher success rate than pattern search method. Also with large initial deviations EMSM costs less steps to find fine alignment spot than pattern search method under the same conditions (see Fig. 11). That means in real operations, pattern search method will generate more errors when the moving steps of pattern search method is much more than that of EMSM. Because pattern search method is a fine aligning algorithm, its result is more stable and accurate while the initial deviation is small. See Fig. 12, with small initial deviations, although pattern search method costs less steps than EMSM, EMSM is more accurate than pattern search method. By contrast, EMSM can be utilized in the condition with much bigger tolerance of errors than pattern search method.

Overall, EMSM is an efficient and high-accurate method to search alignment trajectory. This algorithm can also be used to detect the sensitive movements and sensitive errors on SMP. By doing this, the quality of LWS can be evaluated and the errors can be compensated in a whole different way.

6 Conclusion

In this paper, a geometric error modeling procedure for a typical configuration SMP adopted in LWS is introduced, which is also verified based on topology and multi-body system theory associated with error simulation of mechanical systems. Compared to other methods, a novel EMSM aligning algorithm is proposed. Based on the calculation and experimental results of alignment, some conclusions can be drawn as follows:

1. Error modeling is a feasible method in analyzing the orientation deviations in SMP, and the error propagation pattern can be deduced as well.
2. Error modeling is an efficient way to predict the deviations of different movements, and EMSM is developed to search the optimized alignment trajectory on LWS.
3. This novel algorithm has better performance than pattern search method in several aspects, such as success rate and application range, which is an effective trajectory searching method.

To further improve this error analysis process, sensitivity analysis and error compensation should be taken into account, and EMSM should be developed more in depth in future.

Acknowledgements This research is supported by the Natural Science Foundation of China (Grant No. 51705149), and the Natural Science Foundation of Hunan Province, China (Grant No. 2018JJ3168).

References

1. Yang, H. M., Chen, C. T., Ro, R., et al. (2010). Investigation of the efficient coupling between a highly elliptical Gaussian profile output from a laser diode and a single mode fiber using a hyperbolic-shaped microlens. *Optics & Laser Technology, 42*(6), 918–926.
2. Jedrzejczyk, D., Asbahr, P., Pulka, M., et al. (2014). High-power single-mode fiber coupling of a laterally tapered single-frequency diode laser. *IEEE Photonics Technology Letters, 26*(8), 845–847.
3. Zheng, Y., Li, B., & Duan, J. (2015). Automatic waveguide-fiber alignment algorithm based on polynomial fitting. In *2015 international conference on photonics, optics and laser technology (PHOTOPTICS)* (pp. 77–80).
4. Koganti, P. B., & Udwadia, F. E. (2017). Dynamics and precision control of uncertain tumbling multibody systems. *Journal of Guidance, Control and Dynamics, 40*(5), 1176–1190.
5. Tang, H., Duan, J. A., Lan, S., et al. (2015). A new geometric error modeling approach for multi-axis system based on stream of variation theory. *International Journal of Machine Tools and Manufacture, 92,* 41–51.
6. Chen, G., Li, T., Chu, M., et al. (2014). Review on kinematics calibration technology of serial robots. *International Journal of Precision Engineering & Manufacturing, 15*(8), 1759–1774.
7. Kim, C. K., Lai, M. C., Zhang, Z. C., et al. (2017). Modeling and numerical simulation of afterburning of thermobaric explosives in a closed chamber. *International Journal of Precision Engineering & Manufacturing, 18,* 979.
8. Liu, T., Qian, L., Xu, Y., et al. (2016). Kinematic error modeling and analysis of the loading device based on multi-body theory and stream of variation theory. In *2016 IEEE international conference on information and automation (ICIA), IEEE*.
9. Andolfatto, L., Lavernhe, S., & Mayer, J. R. R. (2011). Evaluation of servo, geometric and dynamic error sources on five-axis high-speed machine tool. *International Journal of Machine Tools and Manufacture, 51*(10–11), 787–796.
10. Li, X., Zhao, H., Zhao, X., et al. (2017). Contouring compensation control based on high accuracy contour error estimation for multi-axis motion systems. *International Journal of Advanced Manufacturing Technology, 93,* 1–11.
11. Tang, H., Duan, J. A., & Lu, S. (2017). Stream-of-variation (SOV) theory applied in geometric error modeling for six-axis motion platform. *IEEE Transactions on Systems Man & Cybernetics Systems, 99,* 1–9.
12. Ibaraki, S., Goto, S., Tsuboi, K., et al. (2018). Kinematic modeling and error sensitivity analysis for on-machine five-axis laser scanning measurement under machine geometric errors and workpiece setup errors. *The International Journal of Advanced Manufacturing Technology, 96,* 4051–4062.
13. Creamer, J., Sammons, P. M., Bristow, D. A., et al. (2017). Table-based volumetric error compensation of large five-axis machine tools. *Journal of Manufacturing Science and Engineering*. https://doi.org/10.1115/1.4034399.
14. Zhao, D., Bi, Y., & Ke, Y. (2017). An efficient error compensation method for coordinated CNC five-axis machine tools. *International Journal of Machine Tools and Manufacture, 123,* 105–115.
15. Xin, L. (2010). Kinematic error modeling for tailored blank laser welding machine based on the improved MBS. *Journal of Mechanical Engineering, 46*(2), 61.
16. Chen, J. X., Lin, S. W., & Zhou, X. L. (2016). A comprehensive error analysis method for the geometric error of multi-axis machine tool. *International Journal of Machine Tools and Manufacture, 106,* 56–66.
17. Cheng, Q., Zhao, H., Zhang, G., et al. (2014). An analytical approach for crucial geometric errors identification of multi-axis machine tool based on global sensitivity analysis. *The International Journal of Advanced Manufacturing Technology, 75,* 107–121.
18. Lee, R. S. (2012). Applying bidirectional kinematics to assembly error analysis for five-axis machine tools with general orthogonal

configuration. *The International Journal of Advanced Manufacturing Technology, 62*(9–12), 1261–1272.
19. Chun, J., Wu, Y., Dai, Y., et al. (2005). Study on automatic alignment technique in fiber active devices packaging. *China Mechanical Engineering*, *16*(24), 2163–2167.
20. Zhao, J. L., Liu, Y., Guo, Z., et al. (2015). Error analysis on CNC gear hobbing machine spindle transmission chain based on SOV theory. *International conference on advanced engineering materials and technology*,. https://doi.org/10.2991/icaemt-15.2015.42.
21. Jee, S. (2012). Real-time inertia compensation for multi-axis CNC machine tools. *International Journal of Precision Engineering & Manufacturing, 13*(9), 1655–1659.
22. Qazani, M. R. C., Pedrammehr, S., & Nategh, M. J. (2018). An investigation on the motion error of machine tools' hexapod table. *International Journal of Precision Engineering & Manufacturing, 19*(4), 463–471.
23. Aguado, S., Samper, D., Santolaria, J., et al. (2012). Towards an effective identification strategy in volumetric error compensation of machine tools. *Measurement Science & Technology, 23*(6), 065003.
24. Zhang, E. Z., Zhao, J., Ji, S. J., et al. (2015). Comprehensive error modeling and compensation for precision polishing platform based on orthogonal experiment and interpolation algorithm. *Guangxue Jingmi Gongcheng/Optic and Precision Engineering, 23*(12), 3422–3429.
25. Kilikevičius, A., & Kasparaitis, A. (2017). Dynamic research of multi-body mechanical systems of angle measurement. *International Journal of Precision Engineering & Manufacturing, 18*(8), 1065–1073.
26. Zeng, W., & Rao, Y. (2019). Modeling of assembly deviation with considering the actual working conditions. *International Journal of Precision Engineering & Manufacturing*, *20*(5), 791–803.
27. Du, S., Yao, X., Huang, D., et al. (2015). Three-dimensional variation propagation modeling for multistage turning process of rotary workpieces. *Computers & Industrial Engineering, 82,* 41–53.
28. Suruga Seiki Corporation. Suruga Fiber Alignment Information: Alignment System. http://eng.surugaseiki.com/alignment.

Publisher's Note Springer Nature remains neutral with regard to jurisdictional claims in published maps and institutional affiliations.

Hao Tang was born in Changsha, Hunan, China, in 1988. He graduated from Dong Hua University, Shanghai, China, and started the M.S. degree in mechanical engineering in Central South University, Changsha, China, in 2009, and transferred into Ph.D student in 2011. His research interests include error analysis, error modeling and precision transferring in complicated multi-axis motion system, and applications of optoelectronic packaging system and laser welding system. He, as a visiting student, went to University of Michigan, Ann Arbor, US, from Sept. 2013 to Mar. 2015, and worked in S.M. Wu manufacture center.

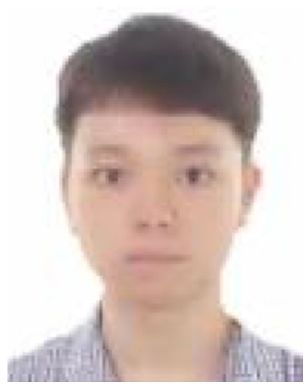

Zilin Zhang is an undergraduate student of Mechanical Engineering at Hunan University of science & technology, China. His research interests include error analysis, error modeling and precision transferring in complicated multi-axis motion system, and applications of optoelectronic packaging system and laser welding system.

Changping Li is an assistant Professor of Mechanical Engineering at Hunan University of science & technology, China. He received his bachelor's from Kumoh National Institute of technology, South Korea. He received master's degrees and Ph.D. in Mechanical Engineering from Yeungnam University, South Korea. His research interests include the development of machine tools; hybrid machining; nontraditional machining; the deburring process of CFRP composites.

Tae Jo Ko is a Professor of Mechanical Engineering at Yeungnam University, South Korea. He received his bachelor's and master's degrees from Pusan National University, South Korea. He received a Ph.D. in Mechanical Engineering from POSTECH, South Korea. His research interests include the development of machine tools; micro-cutting processes; nontraditional machining; surface texturing using piezoelectric actuators; surface texturing using grinding, bio-machining, and textured surfaces on cutting tools; and the deburring process of CFRP composites.